Inorg. Chem. **2006**, *45*, 4170–4176

Synthesis, Isolation, and Structural Characterization of the C_{4h} Isomer of Metal(1,2-naphthalocyanine) and Its One-Dimensional Conductor of the Axially Substituted Species

Eduardo H. Gacho,[†] Hiroyuki Imai,[†] Ryo Tsunashima,[†] Toshio Naito,[†] Tamotsu Inabe,*[,†] and Nagao Kobayashi[‡]

Division of Chemistry, Graduate School of Science, Hokkaido University, Sapporo 060-0810, Japan, and Department of Chemistry, Graduate School of Science, Tohoku University, Sendai 980-8578, Japan

Received December 1, 2005

The C_{4h} isomer of the 1,2-Nc (1,2-naphthalocyaninato) ligand has been efficiently isolated as a hydrated magnesium complex by the fractional crystallization from the benzene/acetone solution after treating the crude mixture of the four isomers (C_{4h}, C_s, C_{2v}, D_{2h}) with benzene. The C_{4h} symmetry has been confirmed by X-ray structure analysis. The central metal ion has been demetalated and subsequently converted to the Li_2 complex followed by conversion to the cobalt(II) complex. Electrochemical oxidation of the Co^{III}(1,2-Nc)$(CN)_2$ anion prepared from the cobalt(II) complex with TPP (tetraphenylphosphonium) has yielded a partially oxidized salt, TPP[Co^{III}(1,2-Nc-C_{4h})$(CN)_2$]$_2$. The crystal comprises slipped stacked Co^{III}(1,2-Nc-C_{4h})$(CN)_2$ one-dimensional chains and one-dimensional arrays of TPPs. The conductivity at room temperature is 0.1 S cm^{-1}, and the temperature dependence is semiconducting with a small activation energy of about 0.05 eV. The positive temperature-independent value of about 60 μV deg^{-1} observed in the thermoelectric power measurements suggests that the salt is in the correlated hopping regime.

Introduction

Phthalocyanines have been known as a functional dye, and their semiconducting electrical properties were noted in as early as 1948.[1] As organic conductors were developed, phthalocyanines have been utilized as a component of molecular[2] and axially bridged polymeric[3,4] conductors with one-dimensional columnar structure and neutral radical conductors.[5] Besides them, axially substituted phthalocyanines, M(Pc)$(CN)_2$; where M = Co^{III} and Fe^{III}, Pc = phthalocyaninato, were also found to be a promising component of molecular conductors.[6−14] The linear extension of the π-ligand yields 2,3-naphthalocyanine (2,3-Nc) derivatives, and Co^{III}(2,3-Nc)$(CN)_2$ has been found to give conducting neutral radical crystals.[15,16] Compared with the linear extension, angular extension of the π-ligand is much more complicated; the conventional synthetic route produces four isomers (C_{4h}, C_s, C_{2v}, D_{2h}: Scheme 1) simultaneously; however, isolation is rather difficult. Among them, the C_{4h} isomer is expected to maintain the planar structure and to give a uniform and efficient $\pi-\pi$ stacking interaction when

* To whom correspondence should be addressed.
[†] Hokkaido University.
[‡] Tohoku University.

(1) Eley, D. D. *Nature* **1948**, *162*, 819.
(2) Inabe, T.; Tajima H. *Chem. Rev.* **2004**, *104*, 5503, and references therein.
(3) Marks, T. J. *Angew. Chem., Int. Ed. Engl.* **1990**, *29*, 857.
(4) Hanack, M.; Datz, A.; Fay, R.; Fischer, K.; Keppeler, U.; Koch, J.; Metz, J. Mezger, M.; Schneider, O.; Schulze, H.-J. *Handbook of Conducting Polymers*; Skotheim, T. A., Ed.; Marcel Dekker: New York, 1986.
(5) Turek, P.; Petit, P.; Andore, J. J.; Simon, J.; Even, R.; Boudjema, B.; Guillaud, G.; Maitrot, M. *J. Am. Chem. Soc.* **1987**, *109*, 5119.
(6) Inabe, T. *J. Porphyrins Phthalocyanines* **2001**, *5*, 3.
(7) Morimoto, K.; Inabe, T. *J. Mater. Chem.* **1995**, *5*, 1749.
(8) Hasegawa, H.; Naito, T.; Inabe, T.; Akutagawa, T.; Nakamura, T. *J. Mater. Chem.* **1998**, *8*, 1567.
(9) Takano, S.; Naito, T.; Inabe, T. *Chem. Lett.* **1998**, 1249.
(10) Fujita, A.; Hasegawa, H.; Naito, T.; Inabe, T. *J. Porphyrins Phthalocyanines* **1999**, *3*, 720.
(11) Matsuda, M.; Naito, T.; Inabe, T.; Hanasaki, N.; Tajima, H.; Otsuka, T.; Awaga, K.; Narymbetov, B.; Kobayashi, H. *J. Mater. Chem.* **2000**, *10*, 631.
(12) Matsuda, M.; Naito, T.; Inabe, T.; Hanasaki, N.; Tajima, H. *J. Mater. Chem.* **2001**, *11*, 2493.
(13) Asari, T.; Naito, T.; Inabe, T.; Matsuda, M.; Tajima, H. *Chem. Lett.* **2004**, *33*, 128.
(14) Asari, T.; Ishikawa, M.; Naito, T.; Matsuda, M.; Tajima, H.; Inabe, T. *Chem. Lett.* **2005**, *34*, 936.
(15) Matsumura, N.; Fujita, A.; Naito, T.; Inabe, T. *J. Mater. Chem.* **2000**, *10*, 2266.
(16) Naito, T.; Matsumura, N.; Inabe, T.; Matsuda, M.; Tajima, H. *J. Porphyrins Phthalocyanines* **2004**, *8*, 1258.

10.1021/ic0520622 CCC: $33.50
Published on Web 04/12/2006

Scheme 1

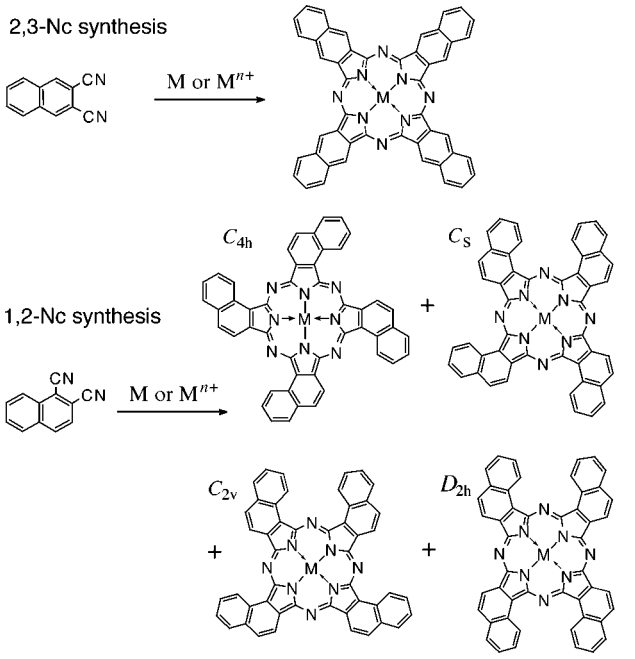

it forms the crystalline conductors by oxidation of the π-ligand.

There have been a few reports on the synthesis and isolation of 1,2-Nc's. While 1,2-Nc's lacking peripheral substituents are generally insoluble, the first successful separation was reported for the C_{4h} isomer of Fe(1,2-Nc)-(isocyanocyclohexyl)$_2$, which was relatively soluble upon complexation with the axial ligand.[17] Recently, Simon et al. reported that each of the four isomers of the magnesium complex can be isolated.[18] The magnesium complexes were relatively soluble in common organic solvents,[19] which enabled isolation by column chromatography; however, it was extremely time-consuming and required excessive amount of solvent to elute the purified complexes. In the current work, the C_{4h} magnesium isomer has been isolated from the crude mixture by fractional crystallization. This method has proven to be remarkably efficient for the C_{4h} isomer. The successful isolation of a preparative amount of the C_{4h} magnesium isomer allowed us to prepare the metal-free species and achieve further metal insertion into this ligand. Thus, the axially substituted compound, (cation)[Co^{III}-(1,2-Nc-C_{4h})(CN)$_2$], has been obtained from the cobalt(II) complex. Electrochemical oxidation of [Co^{III}(1,2-Nc-C_{4h})-(CN)$_2$]$^-$ with tetraphenylphosphonium (TPP) has yielded a conducting partially oxidized salt, TPP[Co^{III}(1,2-Nc-C_{4h})-(CN)$_2$]$_2$, which is analogous to the Pc system, TPP[Co^{III}-(Pc)(CN)$_2$]$_2$. In this paper, preparation, isolation, and structural and optical characterization of the metal complexes of 1,2-Nc-C_{4h} and physical properties of TPP[Co^{III}(1,2-Nc-C_{4h})-(CN)$_2$]$_2$ are presented and compared with the corresponding Pc species.

(17) Hanack, M.; Renz, G.; Strähle, J.; Schmid, S. *Chem. Ber*. **1988**, *121*, 1479.
(18) Negrimovskii, V. M.; Bouvet, M.; Luk'yanets, E. A.; Simon, J. *J. Porphyrins Phthalocyanines* **2000**, *4*, 248.
(19) Bradrook, E. F.; Linstead, R. P. *J. Chem. Soc*. **1936**, 1739.

Experimental Section

Preparation of Mg(1,2-Nc-C_{4h})H$_2$O. A solid mixture of the Mg(1,2-Nc) isomers was prepared as previously described.[18,19] 1,2-Naphthalenedicarbonitrile (4.93 g, 0.0276 mol) was heated with excess Mg metal in a N_2 atmosphere at 375 °C for 2 h. The reaction mixture was cooled to room temperature then heated to around 200 °C under vacuum for 1 h to remove the majority of unreacted 1,2-naphthalenedicarbonitrile. After cooling to room temperature, the remaining solid was finely ground and washed with methylcyclohexane using a Soxhlet extractor for 24 h, and the remaining powder was dried under vacuum. The powder was subsequently stirred in water/ethanol (1:5 in volume) for 2 h. After being filtered and dryed under vacuum, the solid was subjected to extraction with benzene (200 mL) using a Soxhlet extractor for 24 h. Acetone (20 mL) was added to the resultant benzene solution at room temperature, and the dark green solution was left to stand. Purple prism crystals were collected after about 1 week. Addition of a small amount of acetone to the filtrate gave further precipitation of the desired product. The composition of the crystal was determined to be Mg(1,2-Nc-C_{4h})-H$_2$O·(acetone)·3(benzene) on the basis of X-ray structure analysis. Total yield; 0.735 g (17%).

Preparation of H$_2$(1,2-Nc-C_{4h}). The Mg complex obtained was dissolved in concentrated H_2SO_4 and poured through a glass frit onto the crushed ice. The green precipitate identified as H$_2$(1,2-Nc-C_{4h}) by IR spectra was filtered and washed with hot water, methanol, acetone, and ether. Quantitative yield (≥95%).

Preparation of Co^{II}(1,2-Nc-C_{4h}). A solution of butyllithium (1.59 mmol) was added dropwise to a suspension of H$_2$(1,2-Nc-C_{4h}) (0.400 g, 0.56 mmol) in 15 mL of dehydrated DMSO under a N_2 atmosphere. The suspension was then heated to 180 °C and stirred for 30 min. A solution of Co(OAc)$_2$ (1.3 mmol) in DMSO was then added dropwise to the suspension and stirred for 1 h more at 180 °C. After the mixture cooled, distilled water was added slowly. The precipitate was filtered and washed extensively with water, ethanol, and acetone. The solids were then stirred in concentrated H_2SO_4 and poured through a glass frit onto the crushed ice. The precipitate was filtered, washed, and dried. No trace of the H_2 complex was observed in the IR spectra. Yield; 0.39 g (90%).

Preparation of K[Co^{III}(1,2-Nc-C_{4h})(CN)$_2$]. A suspension of Co^{II}-(1,2-Nc-C_{4h})(0.21 g, 0.27 mmol) and KCN (0.40 g, 6.14 mmol) in ethanol (50 mL) was stirred at 60 °C for 72 h (open to the air). Water was then added to the suspension, and the precipitate was filtered and washed with water. K[Co^{III}(1,2-Nc-C_{4h})(CN)$_2$] was extracted with dry acetone using a Soxhlet extractor. The extracted solution was reduced to one-fifth of the volume and diluted with hexane. The precipitated solids were filtered and dried. ^{1}H NMR spectra confirmed that the product contained a single conformer (Supporting Information). Yield; 0.10 g (43%).

Preparation of Et$_4$N[Co^{III}(1,2-Nc-C_{4h})(CN)$_2$]. A suspension of Co^{II}(1,2-Nc-C_{4h})(0.2 g, 0.26 mmol) and tetraethylammonium cyanide (0.5 g, 3.2 mmol) in dry ethanol (50 mL) was refluxed for 72 h with a $CaCl_2$ tube. The precipitate was filtered and washed with water. Et$_4$N[Co^{III}(Pc)(CN)$_2$] was extracted with dry acetonitrile using a Soxhlet extractor. The extracted solution was reduced to one-fifth of the volume and diluted with hexane. The precipitated solids were filtered and dried. Yield; 0.10 g (40%).

Preparation of TPP[Co^{III}(1,2-Nc-C_{4h})(CN)$_2$]$_2$. An electrochemical cell with a glass frit was filled with an acetonitrile solution containing [Co^{III}(1,2-Nc-C_{4h})(CN)$_2$]$^-$ (0.4 mmol dm^{-3}) and TPP·Br (0.4 mmol dm^{-3}). The solution was left to stand for 12 h at 20 °C without current flow to achieve the equilibrium conditions (some precipitation of the cation exchanged species occurs). A constant

Table 1. Data-Collection Conditions and Crystal Data for Mg(1,2-Nc-C_{4h})H_2O·(acetone)·3(benzene) and TPP[Co(1,2-Nc-C_{4h})$(CN)_2]_2$

compound	Mg(1,2-Nc-C_{4h})H_2O·(acetone)·3(benzene)	TPP[Co-(1,2-Nc-C_{4h})$(CN)_2]_2$
	Crystal Data	
formula	$C_{69}H_{50}N_8MgO_2$	$C_{124}H_{68}N_{20}Co_2P$
fw	1047.51	1986.88
cryst syst	monoclinic	tetragonal
space group	$P2_1/n$	$I4_1/a$
a/Å	18.172(1)	32.511(1)
b/Å	12.780(1)	32.511(1)
c/Å	22.961(1)	8.662(1)
β/°	93.29(1)	90
V/Å^3	5323.9(4)	9155.4(5)
Z	4	4
D_x/g cm^{-3}	1.307	1.441
μ(Mo Kα)/cm^{-1}	0.91	4.50
	Data Collection	
$2\theta_{max}$/°	54.98	54.96
Temp of data collection/K	113	123
no. of reflns		
total	45 423	37 533
unique (R_{int})	11 984 (0.053)	5242 (0.101)
	Refinement	
no. of variables	721	333
R1 [$I > 2.0\sigma(I)$]	0.062	0.066
wR2 (F^2, all data)	0.142	0.119
GOF	1.107	0.822

current of 0.5 μA was applied to two platinum electrodes immersed in the solution in each compartment for 6 days at 20 °C. Needlelike crystals grew on the anode surface as the current flowed. Some unidentified solid products were also deposited on the electrode surface. They were largely noncrystalline and probably byproducts of electrochemical oxidation of [Co^{III}(1,2-Nc-C_{4h})$(CN)_2]^-$. Only the crystalline needles were harvested by filtration. The composition of TPP[Co^{III}(1,2-Nc-C_{4h})$(CN)_2]_2$ was confirmed by X-ray structural analysis. More than 10 crystals were subjected to the diffraction experiments, and all of them were found to have the same unit cell parameters.

X-ray Structure Analyses. Single-crystal X-ray diffraction measurements using an automated Rigaku R-axis RAPID imaging plate diffractometer with graphite-monochromated Mo Kα radiation were performed for the two crystals; Mg(1,2-Nc-C_{4h})H_2O·(acetone)·3(benzene) and TPP[Co^{III}(1,2-Nc-C_{4h})$(CN)_2]_2$. All of the measurements were carried out at a low temperature using cold nitrogen gas flow equipment. The crystal data are summarized in Table 1. The structures were solved by direct methods (SIR-88,[20] SIR-92[21]), and the hydrogen atoms were placed at the calculated ideal positions. A full-matrix least-squares technique with anisotropic thermal parameters for non-hydrogen atoms and isotropic parameters (1.2× of the attached atom) for hydrogen atoms was employed for structural refinement using the teXsan program package.[22]

Measurements. UV−vis spectra were measured for the pyridine solutions on a JASCO Ubest V570 spectrometer. IR spectra for the KBr disk specimen were recorded on a Perkin-Elmer 1600 FTIR spectrometer. ^{1}H NMR measurements for the DMSO-d_6 solutions were performed using a 400 MHz JEOL NMR spectrometer. Electrical conductivity was measured in the temperature range of 85−300 K using a standard four-probe method. The contacts between the crystal and gold lead wires (diameter = 20 μm) were made by a gold paste, and the ohmic behavior was confirmed in the range of the applied current of 1−10 μA. The thermoelectric power measurement was carried out using a system similar to that previously reported.[23] Two heater blocks were separated by 1 mm, and the thermal and electrical contacts between the heater blocks and the sample crystal were made with gold foils (thickness = 1 μm) and a gold paste. The temperature gradient was maintained less than 0.5 °C for the whole temperature range. The emf of the system was calibrated by a standard sample of constantan wire, and the reproducibility was checked for several different crystals.

Results and Discussion

Synthesis and Isolation. The fractional crystallization of the isomer mixture obtained from a direct reaction between 1,2-naphthalenedicarbonitril and $Co_2(CO)_8$ was found to be successful for the isolation of the C_{2v} isomer but not for the C_{4h} isomer.[24] Since the cobalt(II) complex is not satisfactorily soluble, isolation of the C_{4h} isomer is rather difficult, even upon attachment of axial ligands. Bradbrook and Linstead reported that the magnesium complex is relatively soluble in common solvents.[19] Therefore, the target was changed to this complex, and the central metal was intended to be exchanged after the isolation according to the report by Simon et al.[18] Extraction of the pure single isomer from the mixture merely by the solubility difference was not successful, whereas the benzene extraction of the hydrated compound gave a C_{4h}-rich solution. Furthermore, preferential crystallization of the C_{4h} isomer occurred when a small amount of acetone was added to the C_{4h}-rich benzene solution. Upon treatment of the mixture of the four isomers with water/ethanol, the hydration reaction was assumed to go to completion for all the isomers. Asymmetric water coordination to the planar isomers leads to symmetry reduction due to the loss of one plane of symmetry. The isomer with C_{2v} or D_{2h} symmetry maintains another plane of symmetry, and no racemization occurs. High symmetries are thought to be advantageous for fractional crystallization; however, no crystalline products have been obtained for the Mg isomers. This may be attributed to the small content of these isomers.[18] Indeed, when the content of the C_{2v} isomer was rich, the asymmetrically pyridine-coordinated C_{2v} species was preferentially isolated for the Co^{II} complex in the crystalline form.[24]

Hydration of the C_{4h} and C_s isomers, which are the major isomers in Mg(1,2-Nc),[18] leads to racemization, and the point groups change to C_4 and C_1, respectively. The higher symmetry of the former is advantageous in crystallization compared with the irregular shape of the latter. As will be described later, the hydrated magnesium 1,2-Nc-C_{4h} complex crystallizes with benzene and acetone. The benzene molecules can be displaced by pyridine, and the space-filling feature of these solvents seems to be a key in the successful isolation of the C_{4h} isomer by simple fractional crystallization.

(20) Burla, M. C.; Camalli, M.; Cascarano, M.; Giacovazzo, M.; Polidori, C.; Spagna, R.; Viterbo, D. *J. Appl. Cryst.* **1989**, *22*, 389.
(21) Altomare, A.; Burla, M. C.; Camalli, M.; Cascarano, M.; Giacovazzo, M.; Guagliardi, A.; Polidori, C. *J. Appl. Cryst.* **1994**, *27*, 435.
(22) *TeXsan, Crystal Structure Analysis Package*; Molecular Structure Corporation: The Woodlands, TX, 1985 and 1992.
(23) Chaikin, P. M.; Kwak, J. F. *Rev. Sci. Instrum.* **1975**, *46*, 429.
(24) Gacho, H. G.; Naito, T.; Inabe, T.; Fukuda, T.; Kobayashi, N. *Chem. Lett.* **2001**, 260.

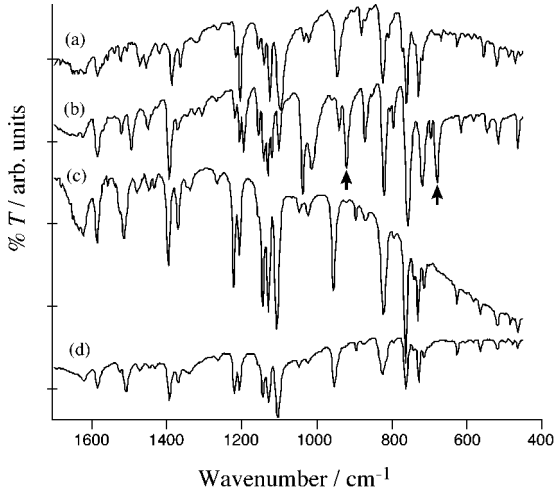

Figure 1. Infrared spectra of (a) Mg(1,2-Nc-C_{4h})H_2O, (b) H_2(1,2-Nc-C_{4h}), (c) Co^{II}(1,2-Nc-C_{4h}), and (d) K[Co^{III}(1,2-Nc-C_{4h})$(CN)_2$]. Arrows in (b) indicate characteristic peaks.

The C_{4h} symmetry of the isolated isomer has been confirmed by X-ray analysis; therefore, further chemical modifications were rather straightforward. After demetalation using a conventional method, several methods were undertaken in an effort to convert the isomer to the cobalt(II) complex. Refluxing H_2(1,2-Nc-C_{4h}) with $CoCl_2$ in quinoline, 1-chloronaphthalene, or DMSO and with $Co_2(CO)_8$ in ethylene glycol did not give a satisfactory yield. The best result was obtained when the metalation was performed with the Li_2 complex following a literature procedure.[18]

The IR spectra of the isolated chemical species are shown in Figure 1. The demetalation from Mg to H_2, as well as metalation from H_2 to Co, was followed by a dramatic change in the spectra. The characteristic peaks of H_2(1,2-Nc-C_{4h}) at 921 and 678 cm^{-1} (indicated by arrows in Figure 1b) may be associated with the N−H out-of-plane deformation and in-plane deformation, respectively. These peaks are observed at 999 and 715 cm^{-1} in H_2(Pc).[25] Two peaks in the region of 1000−1050 cm^{-1} also show characteristic variations by the central chemical species. These features were also utilized to monitor the reaction.

Structure of Mg(1,2-Nc-C_{4h})H_2O·(acetone)·3(benzene). The molecular structure is shown in Figure 2. In this crystal, a Mg(1,2-Nc-C_{4h})H_2O unit is crystallographically independent. As described above, the 1,2-Nc-C_{4h} unit is now a racemic body and the two enantiomers are related by a center of inversion. The Nc ligand is practically planar and the central Mg atom is slightly deviated from the ligand plane (0.497 Å). The bond lengths for the Nc ligand are summarized in Table 2. Compared with the nearly D_{4h} symmetry of the tetraazaporphyrin (TAz) framework in Mg(Pc)H_2O,[26] as indicated by relatively small differences in averaging, C_{4h}-type deformation of the TAz framework in the Mg(1,2-Nc-C_{4h})H_2O unit is detectable: bond e is shortened and bond f is lengthened. This deformation was also observed for Fe(1,2-Nc)(isocyanocyclohexyl)$_2$.[17] The peripheral naphthalene ring maintains the characteristics observed for naphthalene:[27] relatively short bond lengths for n, p, and j. Bond g, which is also short in naphthalene, is not as short because the bond is shared with the TAz ring.

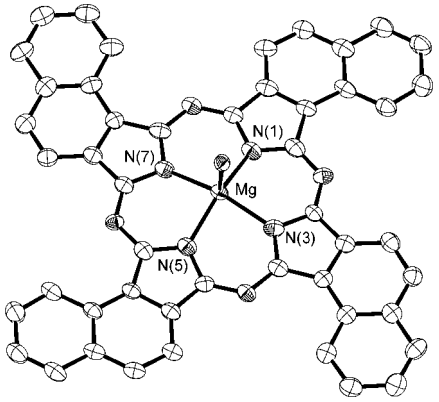

Figure 2. ORTEP drawing of the Mg(1,2-Nc-C_{4h})H_2O unit.

Table 2. Bond Lengths in the 1,2-Nc-C_{4h} Ligand (Å, Averaged by the C_{4h} Symmetry) and in the Pc Ligand (Å, Averaged by the D_{4h} Symmetry)[a]

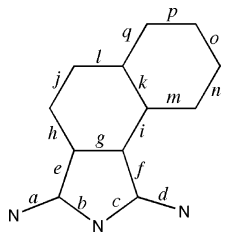

bond	Mg(Pc)H_2O[b]	Mg(1,2-Nc-C_{4h})H_2O	[Co^{III}(1,2-Nc-C_{4h})$(CN)_2$]$^{0.5-}$
a	1.336(7)	1.335(8)	1.316(12)
b	1.367(12)	1.386(8)	1.496(17)
c	1.367(12) (=b)	1.363(6)	1.323(14)
d	1.336(7) (=a)	1.339(5)	1.310(9)
e	1.456(5)	1.437(10)	1.357(9)
f	1.456(5) (=e)	1.463(4)	1.429(28)
g	1.394(6)	1.409(12)	1.474(9)
h	1.391(6)	1.414(11)	1.526(20)
i	1.391(6) (=h)	1.412(11)	1.385(15)
j	1.377(6)	1.360(7)	1.378(15)
k	1.377(6) (=j)	1.420(4)	1.40(3)
l	1.394(6)	1.415(4)	1.36(2)
m	−	1.438(6)	1.45(3)
n	−	1.359(4)	1.31(3)
o	−	1.414(5)	1.54(1)
p	−	1.353(6)	1.32(2)
q	−	1.426(6)	1.42(1)

[a] The values in parentheses are the maximum difference from the average value or the maximum standard deviation. [b] Reference 26.

A portion of the crystal packing is shown in Figure 3. Hydrogen bonds between the axial H_2O and acetone (O···O distances; 2.803(2) and 2.810(2) Å) bridge the two Nc units. Six benzene molecules are packed between the two Nc planes, so that the void between the planes is effectively filled. Therefore, two units of crystallographically independent Mg(1,2-Nc-C_{4h})H_2O·(acetone)·3(benzene), related by a center of inversion, form a relatively condense structural unit that can efficiently crystallize.

(25) Kobayashi, T.; Kurokawa, F.; Uyeda, N.; Suito, E. *Spectrochim. Acta* **1970**, *26A*, 1305.
(26) Fischer, M. S.; Templeton, D. H.; Zalkin, A.; Calvin, M., *J. Am. Chem. Soc.* **1971**, *93*, 2622.
(27) Brock, C. P.; Dunitz, J. D. *Acta Crystallogr., Sect. B* **1982**, *38*, 2218.

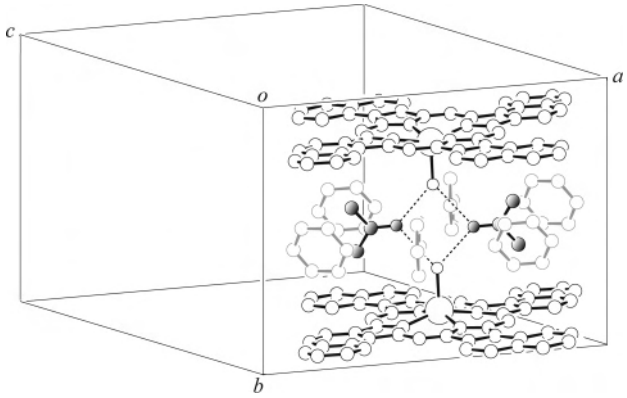

Figure 3. Molecular arrangement of the two Mg(1,2-Nc-C_{4h})H_2O·(acetone)·3(benzene) units in the crystal. Acetone molecules are drawn with shaded spheres, and benzene molecules are drawn in light gray. Broken lines are O−H···O hydrogen bonds.

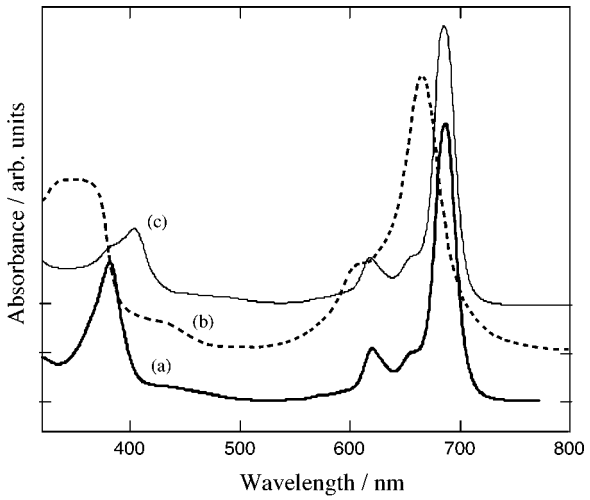

Figure 4. UV−vis spectra of (a) Mg(1,2-Nc-C_{4h})H_2O, (b) Co^{II}(1,2-Nc-C_{4h}), and (c) K[Co^{III}(1,2-Nc-C_{4h})$(CN)_2$] in pyridine.

Table 3. Major Absorption Bands of Pc and Nc Complexes in Pyridine

compound	Soret band/nm	*Q*-band/nm
Mg(1,2-Nc-C_{4h})H_2O	383	688
Mg(Pc)H_2O[a]	347	674
Co^{II}(1,2-Nc-C_{4h})	354	666
Co^{II}(Pc)	333	659
K[Co^{III}(1,2-Nc-C_{4h})$(CN)_2$]	403	685
K[Co^{III}(Pc)$(CN)_2$]	346	675

[a] Reference 29.

Optical Properties. The UV−vis spectra of the Mg, Co^{II}, and Co^{III} complexes in pyridine are shown in Figure 4. The sharp *Q*-band for each compound is consistent with the C_{4h} symmetry of the ligand, as observed in the spectra of the isolated four isomers of Mg(1,2-Nc).[18] The band position is slightly red-shifted compared with that of the corresponding Pc compound (7−14 nm), as shown in Table 3. On the other hand, the Soret bands are largely red-shifted (21−57 nm) compared with those of the corresponding Pc compounds. All these features qualitatively agree with the energy-level shifts expected for the π-extended porphyrinic frameworks; the LUMO is slightly more stabilized than the HOMO, and next-HOMO is largely destabilized in a 1,2-naphthalene-fused porphyrin compared with those in tetrabenzoporphyrin.[28]

Electrochemical Oxidation of [Co(1,2-Nc-C_{4h})$(CN)_2$]$^-$. The cyclic voltammetry of K[Co(1,2-Nc-C_{4h})$(CN)_2$] in DMF showed the first oxidation process at 1.02 V vs Ag/Ag^+. This oxidation corresponds to the π-ligand oxidation observed at 0.96 V for K[Co(Pc)$(CN)_2$]; more positive for 1,2-Nc than for Pc is consistent with the expectation for the angular π-extension of the porphyrinic framework.[28] Since this redox process is not perfectly reversible (nonsymmetrical redox pair with relatively large separation), aggregation may occur near the electrode surface. Therefore, when the applied potential is higher than that of the first oxidation of the π-ligand, electrolysis leads to the crystal growth of the π-radical species. Coexistence of TPP yielded a partially oxidized salt, TPP[Co(1,2-Nc-C_{4h})$(CN)_2]_2$. On the basis of its stoichiometry, the formal charge of the [Co(1,2-Nc-C_{4h})$(CN)_2$] unit was determined to be −0.5; the Nc ligand is oxidized by 1/2*e*.

Crystal Structure of TPP[Co(1,2-Nc-C_{4h})$(CN)_2]_2$. Figure 5a shows the molecular arrangement of the partially oxidized salt. In the analogous Pc conductor, TPP[Co(Pc)$(CN)_2]_2$, the space group is $P4_2/n$.[8] The space group for TPP[Co(1,2-Nc-C_{4h})$(CN)_2]_2$ is changed to $I4_1/a$, and the *Z* value is doubled. In both compounds, however, the Co^{III} ions and the centers of TPP commonly occupy the $\bar{1}$ site and $\bar{4}$ site, respectively. Therefore, one-half of Co(1,2-Nc-C_{4h})$(CN)_2$ and one-quarter of TPP are crystallographically independent. A structural change in the molecular geometry of the 1,2-Nc-C_{4h} ligand upon oxidation could not be clearly seen due to the rather large experimental ambiguity (Table 2).

The 1,2-Nc-C_{4h} units form a one-dimensional chain along the *c* axis, and the TPP cations are also one-dimensionally aligned between the chains. The arrangement of the chains and the TPP arrays are similar to that of TPP[Co(Pc)$(CN)_2]_2$. The structure of the one-dimensional chain is shown in Figure 5b. The 1,2-Nc-C_{4h} rings, which are translationally related along the *c* axis, are stacked with overlaps at two of the four peripheral naphthalene rings with interplanar distance of 3.44 Å. The distance is comparable to that in TPP[Co(Pc)$(CN)_2]_2$.[8] A marked difference between the $\pi-\pi$ overlap in the Pc chain and that in the 1,2-Nc-C_{4h} chain is the relative ring orientation. The chain axis of the Pc chain nearly coincides with one vertical mirror plane of each molecule with D_{4h} symmetry. The same overlap mode is impossible for the 1,2-Nc-C_{4h} chain due to the angular π-extension. The molecule must now be rotated around the CN−Co−CN axis by about 12° to achieve the maximum $\pi-\pi$ overlap (Figure 6a).

The $\pi-\pi$ overlap in the 1,2-Nc-C_{4h} chain is increased compared with that of the Pc chain. However, the degree of $\pi-\pi$ interaction must be considered on the basis of the molecular orbitals. Since the π-ligand is oxidized, the HOMO−HOMO interaction is predominant. The HOMO coefficients were calculated with the structural data using an extended Hückel method, and the overlap integral between the neighboring rings was estimated. The obtained value is 1.8×10^{-3}, which is about one-fifth of that found in TPP-

(28) Kobayashi, N.; Konami, H. *J. Porphyrins Phthalocyanines* **2001**, *5*, 233.

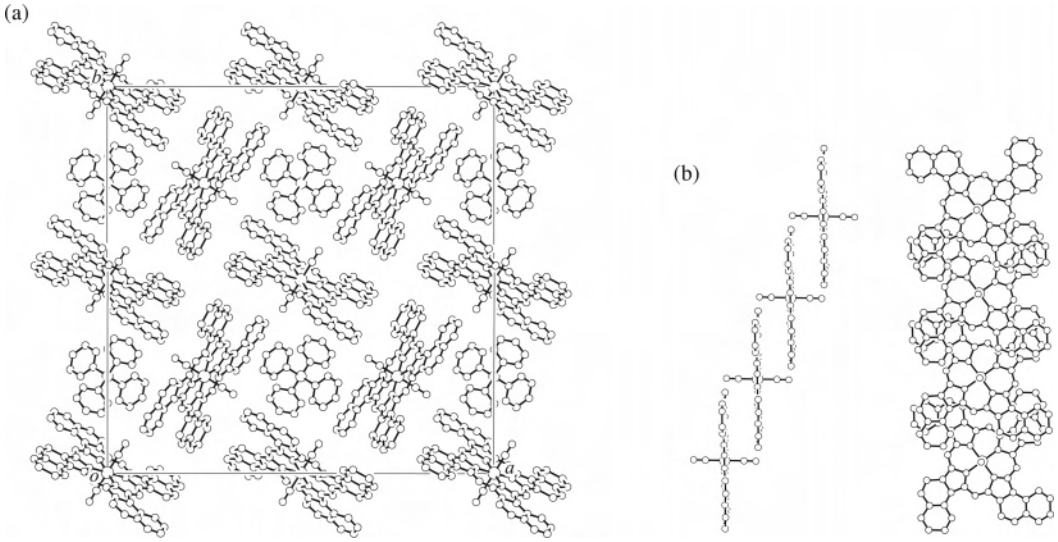

Figure 5. (a) Projection along the *c* axis of the crystal structure of TPP[Co^{III}(1,2-Nc-C_{4h})$(CN)_2$]$_2$. (b) One-dimensional chain of the partially oxidized Co^{III}(1,2-Nc-C_{4h})$(CN)_2$ units.

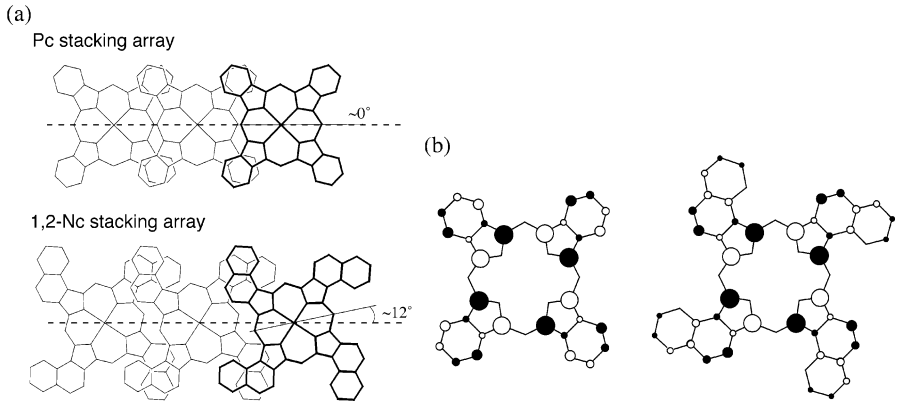

Figure 6. (a) Schematic representation of the molecular orientation in the Pc and 1,2-Nc stacking arrays. (b) Schematic representation of the HOMO coefficients in the Pc and 1,2-Nc ligands.

[Co(Pc)$(CN)_2$]$_2$.[8] Slight rotation of the Pc framework leads to a significant influence on the $\pi-\pi$ interaction. This is thought to be because the HOMO coefficients at peripheral rings are relatively small. In addition, rotation makes the contact between the pyrrole carbon atoms, which have the largest coefficient, in the neighboring 1,2-Nc-C_{4h} rings less efficient (Figure 6b).

Physical Properties of TPP[Co(1,2-Nc-C_{4h})$(CN)_2$]$_2$. The temperature dependence of the single-crystal resistivity (//*c*) of TPP[Co(1,2-Nc-C_{4h})$(CN)_2$]$_2$ is shown in Figure 7. The room-temperature value (9 Ω cm) is about 3 orders of magnitude higher than that of TPP[Co(Pc)$(CN)_2$]$_2$.[8] The temperature dependence is semiconducting with a small activation energy of about 0.05 eV. Since the Nc units form a uniform one-dimensional chain in which the repeat unit coincides with the unit *c* length, the HOMO band is expected to be three/fourths-filled metal-like. The inconsistency between the band picture and the transport behavior may be due to the extremely small overlap integral value, which is approximately proportional to the transfer integral value (*t* = one-quarter of the band width). The bandwidth in TPP[Co(1,2-Nc-C_{4h})$(CN)_2$]$_2$ is estimated as 0.12 eV on the basis of the ratio of overlap integral values in TPP[Co(Pc)$(CN)_2$]$_2$ and TPP[Co(1,2-Nc-C_{4h})$(CN)_2$]$_2$. This value is significantly smaller than the on-site Coulomb repulsion energy (typically 1 eV). Therefore, a simple band picture may not be applied

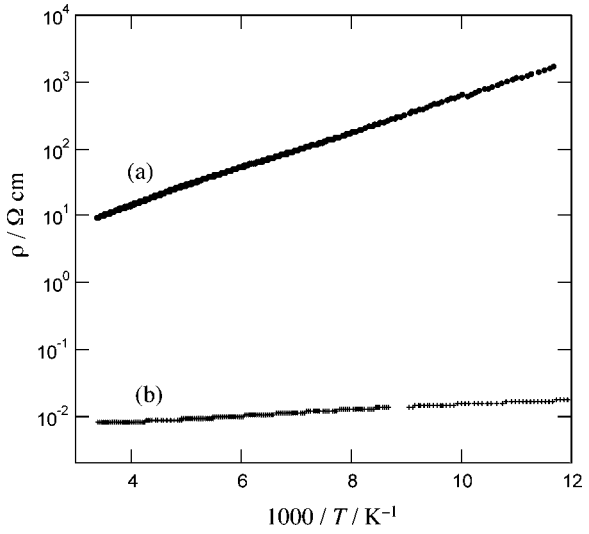

Figure 7. Temperature dependence of the single-crystal electrical resistivity (along the *c* axis) in (a) TPP[Co(1,2-Nc-C_{4h})$(CN)_2$]$_2$ and (b) TPP[Co(Pc)$(CN)_2$]$_2$.

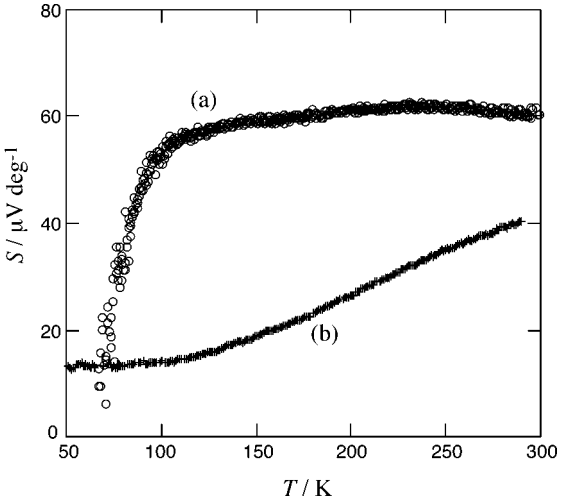

Figure 8. Temperature dependence of the single-crystal thermoelectric power (S; along the c axis) in (a) TPP[Co(1,2-Nc-C_{4h})$(CN)_2]_2$ and (b) TPP-[Co(Pc)$(CN)_2]_2$.

for this system. The similar situation was also observed for TPP[Co(Pc)$(CN)_2]_2$ in which the charge transport is weakly thermally activated though the conduction band is three/fourths-filled metal-like. For this crystal, the charge-ordered (CO) instability due to both on-site and inter-site correlation effects has been suggested.[30,31] TPP[Co(Pc)$(CN)_2]_2$ is thought to be situated at the boundary between metallic and CO states. TPP[Co(1,2-Nc-C_{4h})$(CN)_2]_2$ may be situated completely in an insulating CO regime, since the bandwidth is much narrower than that in the Pc analogue. Therefore, the charge transport is assumed to occur by hopping of localized charges.

The thermoelectric power behavior was also found to be nonmetallic. The temperature dependence of the thermoelectric power (//c) is shown in Figure 8. Above 100 K, the thermoelectric power is constant with a value of about 60 μV deg^{-1}. This behavior can be reproduced by the prediction reported by Chaikin and Beni for the high-temperature limit of the thermoelectric power in a system with a large Coulomb repulsion.[32] According to their paper, the high-temperature limit of the thermoelectric power, $S(T\rightarrow\infty)$, in a system for hole conduction with a large Coulomb repulsion is as follows

$$S(T\rightarrow\infty) = (k_B/e)\ln[2(1-\rho)/\rho],$$

where k_B is the Boltzmann constant, e is the absolute value of the electron charge, and ρ is the ratio of holes to sites. In the present case, ρ is 1/2, leading to $S(T\rightarrow\infty) = 59.7$ μV deg^{-1}. The value is in good agreement with the values we have obtained, suggesting that in TPP[Co(1,2-Nc-C_{4h})$(CN)_2]_2$ the correlation between the charge carriers suppresses their diffusive motion and hopping becomes predominant in charge conduction. Interestingly, the thermoelectric power of TPP[Co(Pc)$(CN)_2]_2$ is clearly metallic; S changes linearly with temperature with a room-temperature value of about 40 μV deg^{-1}. Therefore, the difference again suggests that TPP[Co(Pc)$(CN)_2]_2$ is at the boundary between metallic and CO states and TPP[Co(1,2-Nc-C_{4h})$(CN)_2]_2$ is in an insulating CO regime.

Conclusion

Isolation of a preparative amount of the 1,2-Nc-C_{4h} ligand from the crude mixture, as well as preparation of its partially oxidized one-dimensional conductor of axially CN ligated species, has been reported. Despite the π-extended feature compared with Pc, the $\pi-\pi$ stacking interaction was observed to be considerably reduced. Thus, the conductivity showed apparent semiconducting behavior, and the thermoelectric power indicated a Coulomb repulsion limited constant value. The behavior may be explained by the CO instability in a one/fourth-(hole)filled one-dimensional conductor. Structural analysis did not indicate CO periodicity; however, the extremely small t value in TPP[Co(1,2-Nc-C_{4h})-$(CN)_2]_2$ may be preferable for such a charge localized ground state compared with diffusive charge in a partially filled metallic band.

Acknowledgment. This work was supported in part by a Grant-in-Aid for Scientific Research from the Ministry of Education, Culture, Sports, Science and Technology of the Japanese Government and a Grant-in-Aid for Scientific Research from the Japan Society for the Promotion of Science.

Supporting Information Available: ^{1}H NMR spectra of K[Co-(1,2-Nc-C_{4h})$(CN)_2$] in DMSO-d_6 and X-ray crystallographic files in CIF format for Mg(1,2-Nc-C_{4h})H_2O·(acetone)·3(benzene) and TPP[Co^{III}(1,2-Nc-C_{4h})$(CN)_2]_2$. This material is available free of charge via the Internet at http://pubs.acs.org.

IC0520622

(29) Whalley, M., *J. Chem. Soc*. **1961**, 866.
(30) Seo, H.; Hotta, C.; Fukuyama, H. *Chem. Rev*. **2004**, *104*, 5005.
(31) Hotta, C.; Ogata, M.; Fukuyama, H. *Phys. Rev. Lett*. **2005**, *95*, 216402.
(32) Chaikin, P. M.; Beni, G. *Phys. Rev. B* **1976**, *13*, 647.